Ocean Systems Engineering, *Vol. 6, No. 1 (2016) 117-128*
DOI: http://dx.doi.org/10.12989/ose.2016.6.1.117

Boussinesq equations for internal waves in a two-fluid system with a rigid lid

Chi-Min Liu*

Division of mathematics, General Education Center, Chienkuo Technology University, Changhua City, Taiwan

(Received December 14, 2015, Revised March 2, 2016, Accepted March 7, 2016)

Abstract. A theoretical study of Boussinesq equations (BEs) for internal waves propagating in a two-fluid system is presented in this paper. The two-fluid system is assumed to be bounded by two rigid plates. A set of three equations is firstly derived which has three main unknowns, the interfacial displacement and two velocity potentials at arbitrary elevations for upper and lower fluids, respectively. The determination of the optimal BEs requires a solution of depth parameters which can be uniquely solved by applying the Padé approximation to dispersion relation. Some wave properties predicted by the optimal BEs are examined. The optimal model not only increases the applicable range of traditional BEs but also provides a novel aspect of internal wave studies.

Keywords: internal wave; Boussinesq equations; rigid-lid boundary; two-fluid system

1. Introduction

Internal waves frequently occur in ocean in which the density is stratified due to either temperature or salinity variations. They play an important role in the transport of momentum and energy within the ocean. Based on many observations in marginal seas, for example, the Andaman Sea by Osborne and Burch (1980), it is found that the stratified fluids can be simulated by a two-fluid system as the upper and lower densities of ocean are so close and clearly divided by the pycnocline. Furthermore, such a slight difference in densities of two layers yields a minimal displacement at free surface. Therefore the free surface is commonly replaced by a rigid-lid boundary for simplification and without loss of accuracy.

For linear internal waves, Lamb (1932) displayed the dispersion relations for internal waves in a two-fluid system with a free-surface and rigid-lid boundaries, respectively. Nowadays these solutions are still widely applied to study motions of infinitesimal-amplitude internal waves, and are used to verify the linear properties of nonlinear models. Among nonlinear wave models (see Liu *et al.* 2008 for detailed reviews), Boussinesq equations which were originally developed for weakly nonlinear waves have been extended in the recent two decades for studying waves propagating from deeper water to shallow water in a single-fluid system (Chen and Liu 1995, Gobbi *et al*. 2000, Madsen and Schäffer 1998, Nwogu 1993, Wei *et al*. 1995). In addition, the concern about the accuracy of Boussinesq ocean model was demonstrated by McDougall *et al.*

*Corresponding author, Professor, E-mail: liu.chimin@gmail.com

http://www.techno-press.org/?journal=ose&subpage=7 ISSN: 2093-6702 (Print), 2093-677X (Online)

(2002).

As for the two-fluid system, Liu *et al.* (2008) derived a new set of BEs with the presence of free surface. Based on the derived equations he analyzed basic wave properties including dispersion relation, particle velocities and second-order wave properties. Later Nguyen and Dias (2008) studied the same problem but a rigid-lid boundary condition is considered. Both mathematical derivation and numerical simulation were performed. Debsarma *et al*. (2010) extended Camassa and Choi's work (1999) to propose a set of fully nonlinear model equations also for a two-layer fluid where the lower fluid depth is infinite. A travelling wave solution was examined to verify their solution. Recently, a asymptotic model was theoretically derived and analyzed by Barros and Choi (2013). Local instability near the maximal displacement and bottom effect were mathematically examined by their model equations. It is clear that, either for surface waves or internal waves, Boussinesq equations are quite crucial not only in academic studies but also in many wave-related applications (Myrhaug and Ong 2012, Cifuentes *et al.* 2015, Dong *et al.* 2012, Shi *et al*. 2013).

As the motion of free surface can be reasonably ignored for most studies of internal waves, a rigid-lid assumption will greatly simplify the mathematical analysis. Hence, in this paper the BEs are derived with the assumption of a rigid-lid. Based on the derived equations, two major analyses are made. The first goal is to determine the optimal BEs by firstly determining the unique solution pair of depth parameters with mathematical methods. Secondly, properties of waves and fluid particles are examined. The organization of present study is as follows. In Section 2, a set of BEs is derived by retaining only the leading-order dispersive effect and making no smallness restriction on the nonlinearity. The optimal BEs and how it is determined are demonstrated in Section 3. In Section 4 wave properties including dispersion relation and particle velocities are examined. Conclusions are made in Section 5.

2. Boussinesq equations for a rigid-lid boundary

Internal waves propagating in a two-fluid system with a rigid-lid plate is schematically depicted in Fig. 1. Both fluids are assumed to be inviscid and immiscible. Densities of the upper and lower fluids are ρ_1 and ρ_2, and the density ratio is defined as $\rho_r \equiv \rho_1/\rho_2 < 1$. Flow in each layer is assumed to be irrotational, implying the existence of two velocity potentials Φ_1 and Φ_2 in the upper and lower layers. For a dimensionless analysis, the following non-dimensional variables are introduced: x and y are the horizontal coordinates scaled by a representative wavenumber k_0. z is the vertical coordinate starting at the undisturbed interface of two layers and pointing upward, scaled by a typical thickness h_0. The undisturbed thicknesses of the upper and lower layers h_1 and h_2 are also scaled by h_0. η denotes the interfacial displacement which is scaled by a representative amplitude a_0. All non-dimensional governing equations and boundary conditions are shown as follows (all non-dimensional symbols are neglected hereafter)

$$\mu^2\nabla^2\Phi_1 + \Phi_{1,zz} = 0 \quad \text{within} \quad \varepsilon\eta \le z \le h_1 \tag{1}$$

$$\mu^2\nabla^2\Phi_2 + \Phi_{2,zz} = 0 \quad \text{within} \quad -h_2 \le z \le \varepsilon\eta \tag{2}$$

$$\Phi_{1,z} = 0 \quad \text{at} \quad z = h_1 \tag{3}$$

$$\Phi_{1,z} = \mu^2\left(\eta_t + \varepsilon\nabla\Phi_1\cdot\nabla\eta\right) \quad \text{at} \quad z = \varepsilon\eta \tag{4}$$

$$\Phi_{2,z} = \mu^2\left(\eta_t + \varepsilon\nabla\Phi_2\cdot\nabla\eta\right) \quad \text{at} \quad z = \varepsilon\eta \tag{5}$$

$$\Phi_{2,z} = -\mu^2\left(\nabla\Phi_2\cdot\nabla h_2\right) \quad \text{at} \quad z = -h_2 \tag{6}$$

$$\rho_r\left\{\Phi_{1,t} + \eta + \frac{\varepsilon}{2}\left[\left(\nabla\Phi_1\right)^2 + \frac{1}{\mu^2}\left(\Phi_{1,z}\right)^2\right]\right\} = \Phi_{2,t} + \eta + \frac{\varepsilon}{2}\left[\left(\nabla\Phi_2\right)^2 + \frac{1}{\mu^2}\left(\Phi_{2,z}\right)^2\right] \quad \text{at} \quad z = \varepsilon\eta \tag{7}$$

where the subscripts $,z$ and $,t$ represent the derivatives with respect to z and t, the symbol ∇ is defined as $\nabla \equiv \left(\partial_x, \partial_y\right)$ and two important parameters, μ and ε, which measure the dispersive effect and the nonlinearity respectively, are defined as $\mu = k_0 h_0$ and $\varepsilon = a_0/h_0$. Integrating Eqs. (1) and (2) with respect to z and taking boundary conditions into account, it yields

$$\nabla\cdot\left[\int_{\varepsilon\eta}^{h_1}\nabla\Phi_1 dz\right] = \eta_t \tag{8}$$

$$\nabla\cdot\left[\int_{-h_2}^{\varepsilon\eta}\nabla\Phi_2 dz\right] = -\eta_t \tag{9}$$

Next, velocity potentials are expanded in terms of μ^2 as

$$\begin{cases}\Phi_1(x,y,z,t) = \sum_{n=0}^{\infty}\mu^{2n}\Phi_{1n}(x,y,z,t)\\ \Phi_2(x,y,z,t) = \sum_{n=0}^{\infty}\mu^{2n}\Phi_{2n}(x,y,z,t)\end{cases} \tag{10}$$

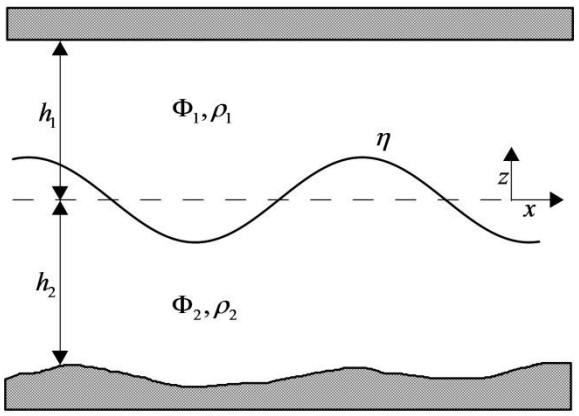

Fig. 1 Internal waves in a two-fluid system with a rigid lid

Substituting Eq.(10) into Eqs. (1), (2), (3) and (6) gives the solutions of Φ_{1n} and Φ_{2n}. Now we introduce two velocity potentials, Φ_U and Φ_L which denote the velocity potentials of the upper and the lower layers at the specific elevations $z = z_U$ and $z = z_L$, respectively. Relations between Φ_1, Φ_2 and Φ_U, Φ_L are

$$\Phi_1 = \Phi_U + \mu^2\left[\frac{z_U^2 - z^2}{2} + h_1(z - z_U)\right]\nabla^2\Phi_U + O(\mu^4) \tag{11}$$

$$\Phi_2 = \Phi_L + \mu^2\left\{\left[\frac{z_L^2 - z^2}{2} - h_2(z - z_L)\right]\nabla^2\Phi_L + (z_L - z)\nabla\Phi_L\cdot\nabla h_2\right\} + O(\mu^4) \tag{12}$$

Substituting Eqs. (11) and (12) into Eqs. (7), (8) and (9) generates the Boussinesq equations expressed in terms of Φ_U, Φ_L and η as

$$-\eta_t + h_1\nabla^2\Phi_U + \mu^2\left(\frac{z_U^2 h_1}{2} - z_U h_1^2 + \frac{h_1^3}{3}\right)\nabla^2\nabla^2\Phi_U - \varepsilon\nabla\cdot(\eta\nabla\Phi_U) + O(\varepsilon^2, \varepsilon\mu^2, \mu^4) = 0 \tag{13}$$

$$\begin{aligned}&\eta_t + h_2\nabla^2\Phi_L + \mu^2\left(\frac{z_L^2 h_2}{2} + z_L h_2^2 + \frac{h_2^3}{3}\right)\nabla^2\nabla^2\Phi_L + \mu^2\left(z_L h_2 + \frac{h_2^2}{2}\right)\nabla\cdot\nabla(\nabla\Phi_L\cdot\nabla h_2)\\ &+ \varepsilon\nabla\cdot(\eta\nabla\Phi_L) + O(\varepsilon^2, \varepsilon\mu^2, \mu^4) = 0\end{aligned} \tag{14}$$

$$\begin{aligned}&(\rho_r - 1)\eta + \rho_r\Phi_{U,t} - \Phi_{L,t} + \mu^2\left[\rho_r\left(\frac{z_U^2}{2} - z_U h_1\right)\nabla^2\Phi_{U,t} - \left(\frac{z_L^2}{2} + z_L h_2\right)\nabla^2\Phi_{L,t}\right]\\ &+ \varepsilon\left[\frac{\rho_r}{2}(\nabla\Phi_U)^2 - \frac{1}{2}(\nabla\Phi_L)^2\right] + O(\varepsilon^2, \varepsilon\mu^2, \mu^4) = 0\end{aligned} \tag{15}$$

where higher-order nonlinear terms are neglected for simplicity. It is remarked that if one adopted Eq. (4) or Eq. (5) instead of using Eq. (3) or Eq. (6) for deriving the equations, some higher-order terms will be different in Eqs.(13) to (15). But such a difference will not affect the determination of the optimal BEs analyzed in the following section. Moreover, Eqs. (13) to (15) can be reduced to some existing wave equations. For example, by keeping Eqs. (14) and (15), retaining the terms of $O(\mu^2)$ and $O(\varepsilon)$ and setting the density ratio ρ_r to be zero, the BEs for a single-layer fluid, which was referred to Chen and Liu (1995), are recovered

3. The optimal Boussinesq equations

In this section the depth parameters z_U and z_L will be determined to acquire the optimal BEs. Depth parameters dominate not only the type of BEs but also wave properties while simulating wave propagation. If the depth parameters are chosen arbitrarily, one cannot ensure that the resulting BEs still behave excellent in the range of $\mu > 1$. Typically the linear dispersion relation is adopted to provide a way toward the optimal choice. For the sake of simplification, only one-dimensional wave is considered in the following analysis. By assuming that the velocity

potentials Φ_U and Φ_L are proportional to $\exp[i(x-t\omega)]$ and eliminating η from BEs, it gives the linear dispersion relation

$$\omega^2=\frac{(1-\rho_r)h_1h_2}{h_1+\rho_r h_2}\cdot\frac{1-\mu^2\left(\frac{z_U^2}{2}+\frac{z_L^2}{2}-z_Uh_1+z_Lh_2+\frac{h_1^2+h_2^2}{3}\right)}{1-\mu^2\left(\frac{z_u^2}{2}+\frac{z_l^2}{2}-z_Uh_1+z_Lh_2+\frac{h_1^3+\rho_r h_2^3}{3(h_1+\rho_r h_2)}\right)} \tag{16}$$

If one hope to extend the applicable range of present BEs from a shallower configuration to a deeper one, it requires to choose a suitable pair of z_U and z_L to make the linear dispersion relation of BEs identical to that of linear wave theory which is shown (se Lamb 1932)

$$\omega_L^2=\frac{1}{\mu}\cdot\frac{(1-\rho_r)\tanh(\mu h_1)\tanh(\mu h_2)}{\tanh(\mu h_1)+\rho_r\tanh(\mu h_2)} \tag{17}$$

Eq. (17) is now rewritten in the form of the (2,2) Padé approximants

$$\omega_{LP}^2=\frac{(1-\rho_r)h_1h_2}{h_1+\rho_r h_2}\cdot\frac{1+\mu^2\left[\frac{\rho_r h_1^3+h_2^3}{15(\rho_r h_1+h_2)}\right]}{1+\mu^2\left[\frac{\rho_r h_1^3+h_2^3}{15(\rho_r h_1+h_2)}+\frac{h_1h_2(\rho_r h_1+h_2)}{3(h_1+\rho_r h_2)}\right]} \tag{18}$$

Equating two coefficients in the numerator and denominator of Eqs. (16) and (18), only one relation is obtained

$$\frac{z_U^2}{2}+\frac{z_L^2}{2}-z_Uh_1+z_Lh_2=-\frac{h_1^2+h_2^2}{3}-\frac{\rho_r h_1^3+h_2^3}{15(\rho_r h_1+h_2)} \tag{19}$$

which can be also represented as

$$(z_U-h_1)^2+(z_L+h_2)^2=\frac{3(\rho_r h_1^3+h_2^3)+5h_1h_2(h_1+\rho_r h_2)}{15(\rho_r h_1+h_2)} \tag{20}$$

It is clear that Eq. (20) cannot give an unique pair of (z_U,z_L). In Liu *et al.* (2008), the solutions are arbitrarily chosen by only one equation. This can be improved by adding an extra equation

$$h_2z_U+h_1z_L=0 \tag{21}$$

to be solved with Eq. (20) to determine a unique pair of depth parameters. It is noted that The imposed condition Eq. (21) is applied to determine a unique solution pair of (z_U,z_L). The major reason why Eq.(21) is chosen is that the solution pair should be located within the range $0\le z_u\le h_1$ and $-h_2\le z_L\le 0$. In Fig. 2, plots of Eqs. (20) and (21) are respectively shown in solid circle and dash line. The radius of solid circle can be easily found to be less than $\sqrt{h_1^2+h_2^2}$. The determined depth parameters are located at the intersection of solid circle and dash line and are solved to be

$$\begin{cases} \dfrac{z_U}{h_1} = 1 - \sqrt{\dfrac{5h_1^2h_2 + 3h_2^3 + 3\rho_r h_1^3 + 5\rho_r h_1 h_2^2}{15\left(h_1^2 + h_2^2\right)\left(\rho_r h_1 + h_2\right)}} \\ \dfrac{z_L}{h_2} = -1 + \sqrt{\dfrac{5h_1^2h_2 + 3h_2^3 + 3\rho_r h_1^3 + 5\rho_r h_1 h_2^2}{15\left(h_1^2 + h_2^2\right)\left(\rho_r h_1 + h_2\right)}} \end{cases} \tag{22}$$

Eq. (22) can make sure that both of depth parameters will have reasonable values, i.e., $0 \le z_U \le h_1$ and $-h_2 \le z_L \le 0$. Related results are plotted in Fig. 3. Solid and dash curves represent z_U/h_1 and z_L/h_2, respectively. Density ratio $\rho_r = 0.997$ is chosen to meet general condition in real oceans. $h_1 = 1$ is fixed and only the range of $0 < h_2/h_1 < 1$ is considered and plotted for the sake of avoiding the possible divergence while the thickness ratio grows that will be demonstrated in next section. Results show that z_U and z_L respectively are approximately a half of h_1 and h_2.

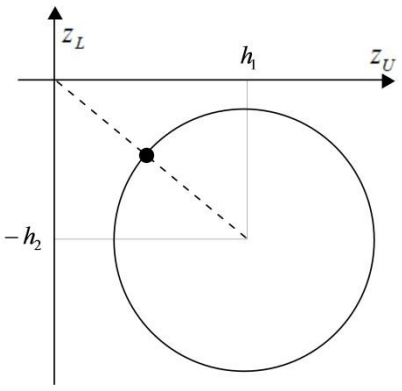

Fig. 2 Solutions of z_U and z_L

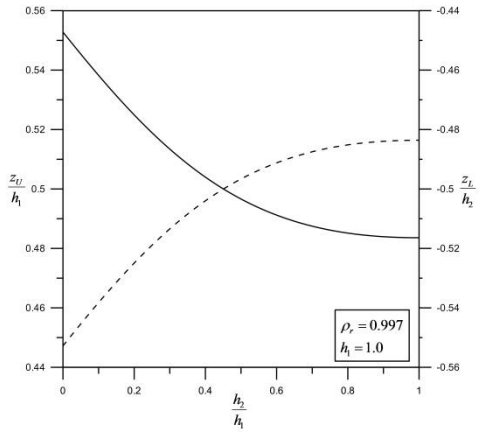

Fig. 3 Relations between (z_U, z_L) and thickness ratio h_2/h_1 for $\rho_r = 0.997$ and $h_1 = 1$

4. Examination of wave properties

Dispersion relation and particle velocities for linear waves will be analyzed in this section. First, the rigid-lid model (present BEs) and the free-surface model (Liu *et al*. 2008) will be compared to verify the feasibility of the former one. Dispersion relation for the free-surface model (see Eq. (18) in Liu *et al*. 2008) is

$$\omega_{Lf}^4 - M\omega_{Lf}^2 + N = 0 \tag{23}$$

where

$$\begin{cases} M = \dfrac{1}{\mu}\cdot\dfrac{\tanh(\mu h_1)+\tanh(\mu h_2)}{1+\rho_r\tanh(\mu h_1)\tanh(\mu h_2)} \\ N = \dfrac{1}{\mu^2}\cdot\dfrac{(1-\rho_r)\tanh(\mu h_1)\tanh(\mu h_2)}{1+\rho_r\tanh(\mu h_1)\tanh(\mu h_2)} \end{cases} \tag{24}$$

Thus two types of wave motions can be readily solved by Eq. (23)

$$\omega_{Lf}^2 = \frac{M}{2}\left(1 \pm \sqrt{1-\frac{4N}{M^2}}\right) \tag{25}$$

where the positive and negative signs denote the fast-mode (surface-mode) and slow-mode (internal-mode) motions, respectively. For internal wave motions, the slow-mode case is considered with the assumption of $\rho_r \sim 1$ for real oceans. It yields

$$\omega_{Lf}^2 \sim \frac{N}{M} = \frac{1}{\mu}\cdot\frac{(1-\rho_r)\tanh(\mu h_1)\tanh(\mu h_2)}{\tanh(\mu h_1)+\tanh(\mu h_2)} \tag{26}$$

Eq. (26) is equivalent to that of the rigid-lid case simplified from Eq. (17)

$$\omega_L^2 \sim \frac{1}{\mu}\cdot\frac{(1-\rho_r)\tanh(\mu h_1)\tanh(\mu h_2)}{\tanh(\mu h_1)+\tanh(\mu h_2)} \tag{27}$$

A comparison of dispersion relation of both cases is depicted in Fig.4. Ratios of Eq. (17) to Eq. (25) are compared under different thickness ratios and relative water depths. A very slight difference between two cases appears. It is also found that the difference in the shallower-water configuration is larger than that in the deeper-water configuration because nonlinear effects become stronger in the former. Above result demonstrates the validity of replacing the free surface by a rigid lid when the density ratio approaches unity.

Next, dispersion relations between present BEs and linear wave theory are shown in Fig. 5. Comparisons of Eq. (16) to Eq. (17) are depicted. Cases of various thickness ratios are examined. A poorer behavior of BEs occurs when the thickness ratio h_2/h_1 becomes larger. To eliminate this flaw, two cases classified by the thickness ratio are introduced

$$\begin{cases} h_1 = 1, \quad h_2 = \delta_1, \quad \text{for} \quad h_1 \geq h_2 \\ h_1 = \delta_2, \quad h_1 = 1, \quad \text{for} \quad h_1 \leq h_2 \end{cases} \tag{28}$$

in which both δ_1 and δ_2 are less than unity to avoid the possible divergence of wave properties, as previously shown in Fig.5. With the help of Eq. (28), frequency ratios of dispersion relations of Eqs. (16) and (17) for both cases are plotted in Fig. 6. Solid and dash curves denote the frequency ratios for cases $h_1 \geq h_2$ (with δ_1 along the bottom coordinate) and $h_1 \leq h_2$ (with δ_2 along the top coordinate), respectively. For a fixed value of μ, results of both cases are almost the same which can be readily seen by Eqs. (16) and (17) when ρ_r approaches unity. Maximum errors are about 10% for the case of $\mu = 5$ and about 37% for those of the case $\mu = 10$. It demonstrates that present BEs can provide a better prediction in regions of larger values of μ than traditional BEs.

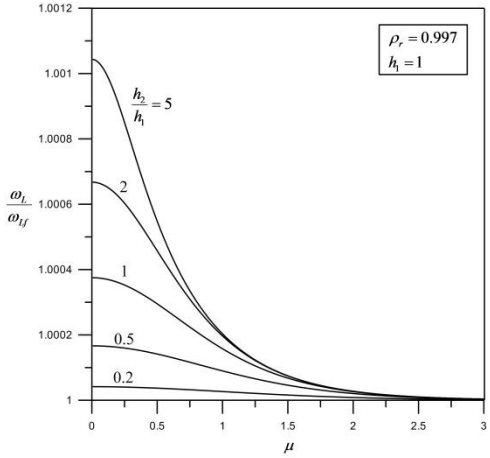

Fig. 4 Comparison of dispersion relations of the free-surface model and present BEs for $\rho_r = 0.997$ and $h_1 = 1$

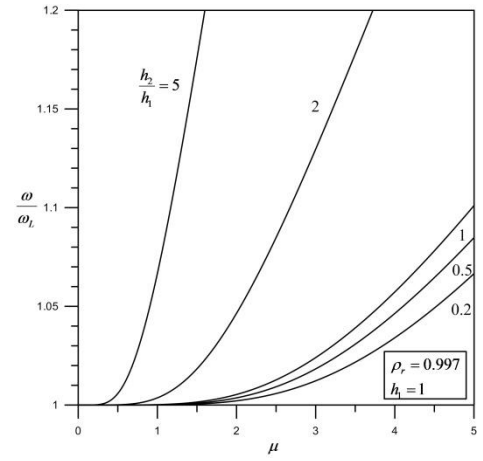

Fig. 5 Relations between ω/ω_L and μ for various values of h_2/h_1 for $\rho_r = 0.997$ and $h_1 = 1$

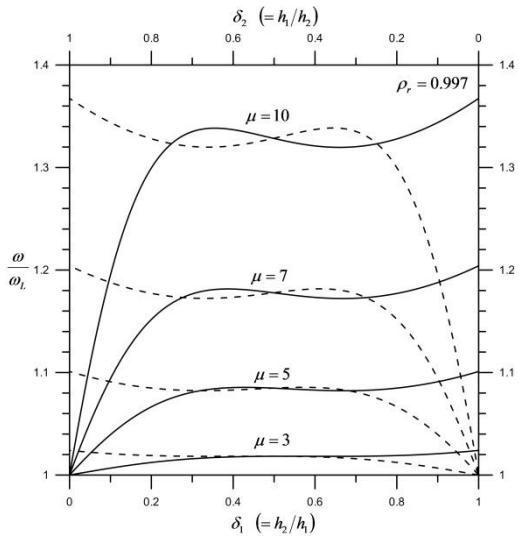

Fig. 6 Relations between ω/ω_L and thickness ratios δ_1 or δ_2. Solid curves for the cases $h_1 > h_2$ and dash curves for the cases $h_1 < h_2$

Next, velocities of water particles are derived and examined. Horizontal velocities for the upper and the lower layers, which are normalized by those at the interface, are

$$HV_1 \equiv \frac{\nabla\Phi_1}{\nabla\Phi_1(z=0)} = \frac{1-\mu^2\left[\frac{z_U^2 - z^2}{2} + h_1(z - z_U)\right]}{1-\mu^2\left[\frac{z_U^2}{2} - h_1 z_U\right]} \tag{29}$$

$$HV_2 \equiv \frac{\nabla\Phi_2}{\nabla\Phi_2(z=0)} = \frac{1-\mu^2\left[\frac{z_L^2 - z^2}{2} - h_2(z - z_L)\right]}{1-\mu^2\left[\frac{z_L^2}{2} + h_2 z_L\right]} \tag{30}$$

Similarly, results for vertical velocities are

$$VV_1 \equiv \frac{\Phi_{1,z}}{\Phi_{1,z}(z=0)} = \frac{\mu^2(-z + h_1)}{\mu^2 h_1} \tag{31}$$

$$VV_2 \equiv \frac{\Phi_{2,z}}{\Phi_{2,z}(z=0)} = \frac{\mu^2(z + h_2)}{\mu^2 h_2} \tag{32}$$

Solutions for linear waves are

$$HV_{1L} = \frac{\cosh \mu(z - h_1)}{\cosh \mu h_1} \tag{33}$$

$$HV_{2L} = \frac{\cosh \mu(z + h_2)}{\cosh(\mu h_2)} \tag{34}$$

$$VV_{1L} = \frac{\sinh \mu(z - h_1)}{-\sinh \mu h_1} \tag{35}$$

$$VV_{2L} = \frac{\sinh \mu(z + h_2)}{\sinh \mu h_2} \tag{36}$$

Now Eqs. (29) to (32) are compared to Eqs. (33) to (36) and results are shown in Fig. 7. Two cases for $\mu = 1$ and $\mu = 2$ are plotted for a fixed thickness ratio $h_1/h_2 = 1$. Solid and dash-dot curves respectively represent the results of horizontal and vertical velocities of present BEs. Solutions predicted by linear wave theory are drawn by short-dash and long-dash curves for horizontal and vertical velocities, respectively. Behaviors of present BEs are very close to those of linear wave theory for the case $\mu = 1$. It is also seen that the deviation also rapidly increases as μ grows. The reason is stemmed from the inefficiency of using present $O(\mu^2)$ model to calculate the particle velocities. A higher-order model is expected to substantially improve the accuracy of particle velocities predicted by BEs.

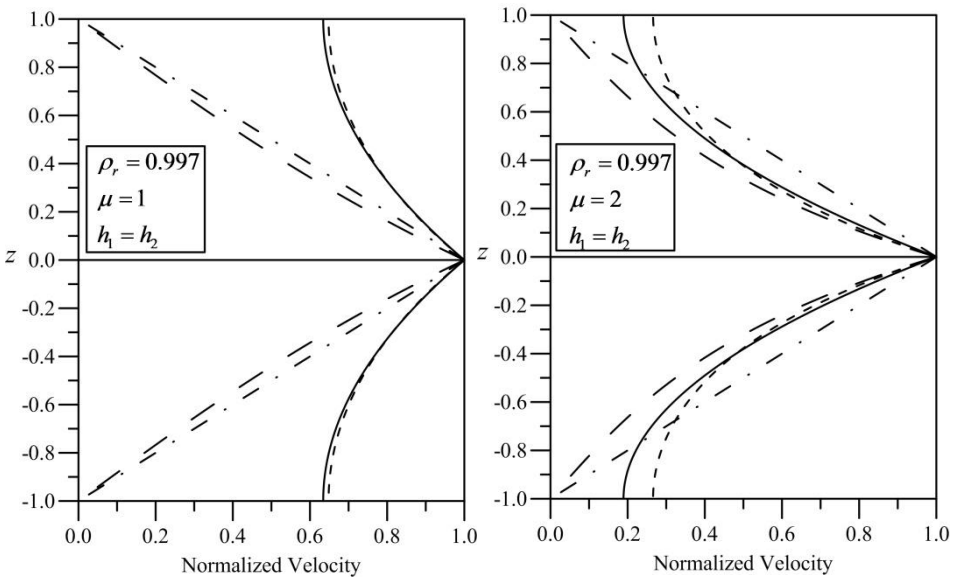

Fig. 7 Comparison between normalized particle velocities of present BEs with those of linear wave theory. Solid, dash-dot, short-dash and long-dash curves respectively represent HV_i, VV_i, HV_{iL} and VV_{iL} ($i = 1,2$) for fixed conditions $\rho_r = 0.997$ and $h_1 = h_2$. (a) cases of $\mu = 1$ and (b) cases of $\mu = 2$

5. Conclusions

Boussinesq equations for internal waves propagating in a two-fluid system bounded by rigid boundaries are mathematically examined in this paper. By incorporating the Padé approximants into the exact linear dispersion relation, the depth parameters z_U and z_L are uniquely determined to acquire the optimal equations. Based on the derived equations, dispersion relation and velocities of fluid particles are compared with those of linear wave theory. Some of wave properties predicted by present equations are good when relative water depth goes large. More excellent and accurate results are expected if a higher-order model is adopted.

Based on present study, numerical simulation can be performed by applying the derived equations and relative results. Comparison with other wave models and further analysis will be carried out in the coming future.

Acknowledgments

The author would like to thank the support by National Science Council of Taiwan with grant no. MOST 104-2221-E-270-003-MY2 and NSC 102-2911-I-006-302.

References

Barros, R. and Choi, W. (2013), "On regularizing the strongly nonlinear model for two-dimensional internal waves", *Physica D*, **264**, 27-34.

Camassa, R. and Choi, W. (1999), "Fully nonlinear internal waves in a two-fluid system", *J. Fluid Mech.*, **396**, 1-36.

Chen, Y. and Liu, P.L.F. (1995), "Modified Boussinesq equations and associated parabolic models for water wave propagation", *J. Fluid Mech*., **288**, 351-381.

Cifuentes, C., Kim, S., Kim, M.H. and Park, W.S. (2015), "Numerical simulation of the coupled dynamic response of a submerged floating tunnel with mooring lines in regular wave", *Ocean Syst. Eng*., **5**(2), 109-123.

Debsarma, S., Das, K.P. and Kirby, J.T. (2010), "Fully nonlinear higher-order model equations for long internal waves in a two-fluid system", *J. Fluid Mech*., **654**, 281-303.

Dong, G.H., Ma, Y.X., Zhang, W. and Ma, X.Z. (2012), "Laboratory study on the modulation evolution of nonlinear wave trains", *Ocean Syst. Eng*., **2**(3), 189-203.

Gobbi, M.F., Kirby, J.T. and Wei, G. (2000), "A fully nonlinear Boussinesq model for surface waves - Part 2. extension to $O(kh)^4$", *J. Fluid Mech*., **405**, 181-210.

Lamb, H. (1932), *Hydrodynamics*, Cambridge Univ. Press, New York, USA.

Liu, C.M., Lin, M.C. and Kong, C.H. (2008), "Essential properties of Boussinesq equations for internal and surface waves in a two-fluid system", *Ocean Eng*., **35**, 230-246.

Liu, P.L.F. and Wang, X. (2012), "A multi-layer model for nonlinear internal wave propagation in shallow water", *J. Fluid Mech*., **695**, 341-365.

Madsen, P.A. and Schäffer, H.A. (1998), "Higher-order Boussinesq-type equations for surface gravity waves: derivation and analysis", *Philos. T. R. Soc. A*, **356**, 3123-3184.

McDougall, T.J., Greatbatch, R.J. and Lu, Y. (2002), "On conservation equations in oceanography: How accurate are Boussinesq ocean models?", *J. Phys. Oceanog*., **32**, 1574-584.

Myrhaug, D. and Org, M.C. (2012), "Scour around spherical bodies due to long-crested and short-crested nonlinear random waves", *Ocean Syst. Eng*., **2**(4), 257-269.

Nguyen, H.Y. and Dias, F. (2008), "A Boussinesq system for two-way propagation of interfacial waves", *Physica D*, **237**, 2365-2389.
Nwogu, O. (1993), "Alternative form of Boussinesq equations for nearshore wave propagation", *J. Wtrwy. Port Coast Ocean Engng. ASCE*, **119**, 618-638.
Osborne, A.R. and Burch, T.L. (1980), "Internal solitons in the Andaman Sea", *Science*, **208**, 451-460.
Shi, S., Kurup, N., Halkyard, J. and Jiang, L. (2013), "A study of internal wave influence on OTEC systems", *Ocean Syst. Eng.*, **3**(4), 309-325.
Wei, G., Kirby, J.T., Grilli, S.T. and Subramanya, R. (1995), "A fully nonlinear Boussinesq model for surface waves. Part 1. Highly nonlinear, unsteady waves", *J. Fluid Mech*., **294**, 71-92.